

# Modeling and Control of the Yaw Channel of a UAV Helicopter

Guowei Cai, *Student Member, IEEE*, Ben M. Chen, *Fellow, IEEE*, Kemao Peng, *Member, IEEE*, Miaobo Dong, and Tong H. Lee, *Member, IEEE*

**Abstract**—We present in this paper the modeling and flight-control-system design for the yaw channel of an unmanned-aerial-vehicle (UAV) helicopter using a newly developed composite nonlinear feedback (CNF)-control technique. The CNF-control method has been proven to be capable of yielding a fast transient response with no or very minimal overshoot in tracking a specific target. From the actual flight tests on our UAV helicopter, it has been found that the commonly used yaw dynamical model for the UAV helicopter proposed in the literature is very rough and inaccurate, which might cause the helicopter to shake severely in certain flight conditions. This motivates us to first obtain a more accurate model for the yaw channel of our UAV helicopter. The CNF-control method is then utilized to design an efficient control law, which gives excellent overall performance. In particular, our design has achieved a Level 1 performance according to the standards set for military rotorcraft. The results are verified through actual flight tests.

**Index Terms**—Aircraft control, modeling, nonlinear control, unmanned-aerial-vehicle (UAV) helicopters.

## I. INTRODUCTION

UNMANNED aerial vehicles (UAVs) have recently gained much attention in the academic circle worldwide. They have potential military and civil applications as well as scientific significance in the academic research. The UAV, in particular, the unmanned helicopter, can serve as an excellent platform for studying plants with maneuverability and versatility. Many research groups are constructing their own UAV helicopter platforms for their research purposes (see, e.g., [3], [10], [16], and [18]). A number of system identification methods have been proposed to derive linear or nonlinear model for specific flight conditions or envelope (see, e.g., [13], [16], and [19]). Many control techniques (see, e.g., [2], [12], and [20]) are also employed to implement automatic flight control systems on UAV helicopters.

Our motivation in developing a UAV helicopter is to build a test bed for implementing some newly developed linear and nonlinear control techniques, particularly, the composite non-



Fig. 1. UAV helicopter, HeLion.

linear feedback (CNF) control, which has proven to be capable of yielding a very fast transient response with no or very minimal overshoot. The CNF-control technique was first introduced by Lin *et al.* [14] to improve the tracking performance under state-feedback laws for a class of second-order systems subject to actuator saturation. Recently, it has been fully developed to handle general systems with input constraints and with measurement feedback (see, e.g., Chen *et al.* [6], [7]) and applied to design a high-performance positioning mechanism for an XY table [8]. The CNF control consists of a linear-feedback law and a nonlinear-feedback law without any switching element. The linear-feedback part is designed to yield a closed-loop system with a small damping ratio for a quick response, while at the same time, not exceeding the actuator limits for the desired command-input levels. The nonlinear-feedback law is used to increase the damping ratio of the closed-loop system as the system output approaches the target reference to reduce the overshoot caused by the linear part. The design philosophy of the CNF technique is on reducing overshoot and speeding up its settling time of the overall control system.

We have recently constructed a small-scale UAV helicopter platform, called HeLion. Shown in Fig. 1 is HeLion upgraded from a radio-controlled hobby helicopter, Raptor 90. To realize automatic flight control [4] of the UAV, we have designed and integrated an avionic system to the bare helicopter. The system includes the following features: 1) an airborne computer system for collecting data, executing flight control laws, driving actuators, and communicating with a ground supporting system; 2) necessary sensors for measuring signals and actuators used for driving control surfaces; 3) a communication system for providing wireless communications between the onboard system and the ground supporting system; 4) an airborne

Manuscript received January 19, 2008; revised May 22, 2008. Published August 29, 2008 (projected). This work was supported in part by the Defence Science and Technology Agency (DSTA) of Singapore under the 2003 Temasek Young Investigator Award.

G. Cai, B. M. Chen, M. Dong, and T. H. Lee are with the Department of Electrical and Computer Engineering, National University of Singapore, Singapore 117576 (e-mail: caiguowei@nus.edu.sg; bmchen@nus.edu.sg; bmchen@ieee.org; eledm@nus.edu.sg; eleleth@nus.edu.sg).

K. Peng is with Temasek Laboratories, National University of Singapore, Singapore 117508 (e-mail: kmpeng@nus.edu.sg).

Color versions of one or more of the figures in this paper are available online at <http://ieeexplore.ieee.org>.

Digital Object Identifier 10.1109/TIE.2008.926780

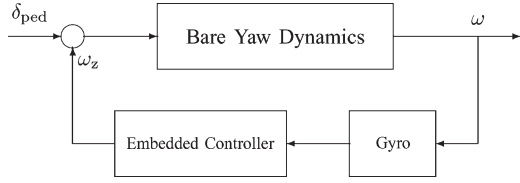


Fig. 2. Configuration of the yaw channel of the UAV helicopter.

power-supply system; and 5) a ground supporting computer system [9] for scheduling flight paths and collecting in-flight data. A linearized model, which has a similar structure as that proposed in [16], for hover or near-hover flight condition is obtained, and an automatic control law using the CNF-control method has been implemented on the actual UAV helicopter [5]. The implementation is quite successful. However, performance on certain aspects is not as good as expected. In particular, we have found that the commonly used dynamical model for the yaw channel is very rough and inaccurate, particularly in the relative high-frequency region (above 4 Hz in HeLion), which is seldom stimulated by manual control. Such inaccuracy causes the helicopter to shake severely on many occasions during the actual flight tests.

To improve the overall performance, we carry out in this paper the modeling process to obtain a more accurate dynamical model for the yaw channel. We have found a mathematical model that gives a much more accurate response. The CNF-control technique is then utilized to design a high-performance flight control law with excellent performance. In particular, our design has achieved a Level 1 performance according to the standards set for military rotorcraft. The results have been verified through simulation and actual flight tests.

The outline of this paper is as follows. In Section II, we present a comprehensive procedure for deriving the dynamical model of the yaw channel of our UAV helicopter. In Section III, the CNF-control technique is used to design the flight control law based on the model obtained in Section II. Simulation and actual implementation results, as well as the analysis on the overall performance, are given in Section IV to verify the superiority of the designed controller. Finally, in Section V, we will draw some concluding remarks.

## II. MODELING OF UAV YAW-CHANNEL DYNAMICS

It is well known that yaw direction control is one of the most challenging jobs in controlling small-scale UAV helicopters. Due to the small size of hobby helicopter such as Raptor 90, the torque associated with the yaw channel is highly sensitive. As a result, signals including small amplitude input, wind-gust disturbance, and slight change of torque in the main rotor may produce a large change in yaw rate and make the manual hovering of a traditional hobby helicopter extremely difficult. To overcome such a problem, modern hobby helicopters are commonly equipped with a yaw rate gyro, which consists of a low-cost yaw-angular-rate sensor and a simple controller to stabilize the yaw rate and/or heading angle. The block diagram of the control configuration is shown in Fig. 2. For our HeLion UAV helicopter, a Futaba GY601 heading-lock gyro with an exclusive digital servo S9251 is used. Such a rate gyro is praised to be capable of providing the best yaw rate and angle stabilization

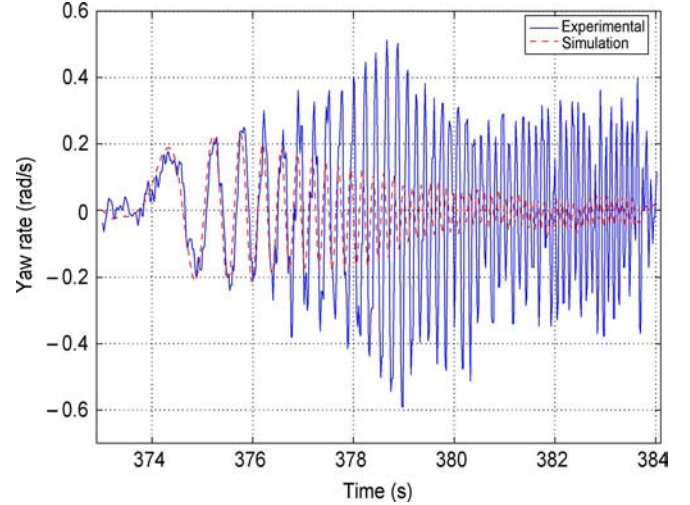


Fig. 3. Time-domain verification of the conventional second-order model for the yaw channel.

in manual maneuvering. It, however, still has problems when it comes to high-precision control on yaw rate and heading angle. To enhance the performance of the yaw channel, a more accurate model characterizing the input–output relationship of the channel is necessary.

In Fig. 2,  $\delta_{ped} \in [-1, 1]$  is the normalized input to the yaw channel.  $\omega$  is the yaw rate in radians per second, which can be measured either by a yaw rate gyro or an inertial measurement unit, and  $\omega_z$  is the output signal of the embedded controller. Traditionally, the identification of this model is based on two important assumptions (see, e.g., [16]): 1) The simplified bare yaw dynamics is a first-order system, and 2) the embedded controller is characterized by a first-order low-pass filter

$$\frac{\omega_z}{\omega} = \frac{K_\omega}{s + K_{\omega_z}} \quad (1)$$

where  $K_\omega$  and  $K_{\omega_z}$  are the unknown parameters. For our UAV helicopter, HeLion, we manage to identify a simplified model in the state-space form and is given as

$$\begin{pmatrix} \dot{\omega} \\ \dot{\omega}_z \end{pmatrix} = \begin{bmatrix} -5.5561 & -36.6740 \\ 2.7492 & -11.1120 \end{bmatrix} \begin{pmatrix} \omega \\ \omega_z \end{pmatrix} + \begin{bmatrix} 58.4053 \\ 0 \end{bmatrix} \delta_{ped}. \quad (2)$$

This model works pretty well for manual control, and its feasibility has been proved by manual-flight tests and automatic-hovering tests in [5]. However, it is found that the accuracy of such a model is not acceptable for high-bandwidth flight control. Figs. 3 and 4 show, respectively, the time- and frequency-domain verifications of the identified model together with the actual response of the system. It can be clearly observed that the traditional model yields a poor performance in the high-frequency region. This motivates us to carry out a modeling process to identify a more accurate model for the yaw channel of our UAV helicopter.

To ensure the quality of data, flight experiment has to be carefully designed. In [5], [16], and [19], it has been verified that, for small-scale UAV helicopter, the yaw-channel dynamics can be physically decoupled from other channels in hover and near-hover flight conditions. Thus, it is reasonable to assume

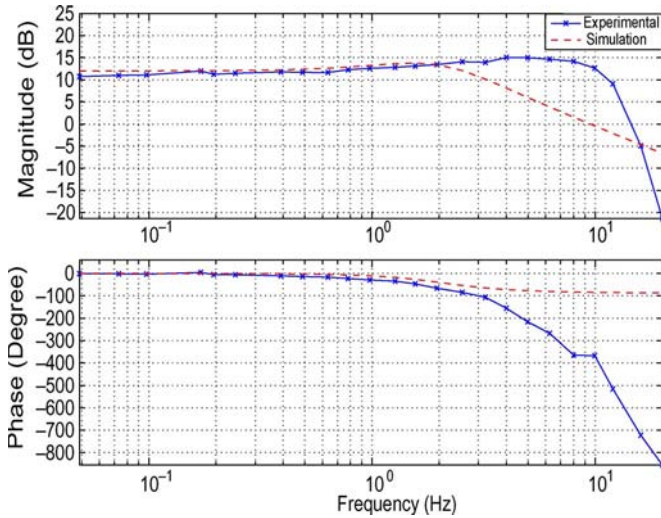


Fig. 4. Frequency-domain verification of the conventional second-order model for the yaw channel.

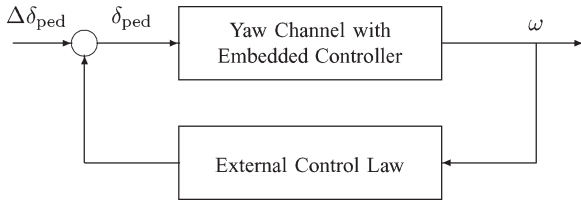


Fig. 5. Schematic diagram of data collection in the closed-loop setting.

that the yaw-channel dynamics is a single-input–single-output (SISO) system.

The data-collection experiment is performed in closed loop, which means that the extra feedback controller is included to ensure the stabilization. To a system like the HeLion UAV, which is inherently unstable, closed-loop experiment is an ideal choice. The feasibility and identifiability of closed-loop identification have been discussed in [15] in detail. Compared with the open-loop experiment, which is conducted under purely manual control, closed-loop experiment has the following two unique advantages.

- 1) With the extra feedback controller, the stability of the identified system is guaranteed, and the augmented system can be fully excited by computer-generated input signal over the interested frequency range, particularly in frequencies above 4 Hz, which is difficult to control manually.
- 2) Since the designed controller is known, the closed-loop identification can be transferred to open-loop identification. Then, all of the identification algorithms which are suitable for open-loop identification can still be used.

The schematic diagram of data-collection experiment in the closed-loop setting is shown in Fig. 5. The bare yaw dynamics augmented with the embedded controller is regarded as a whole system. The additional feedback controller is part of the automatic flight control law designed to stabilize the overall helicopter at the hovering flight condition. When automatic hovering is achieved, we inject a set of sinusoidal signals generated by the onboard computer system into  $\Delta\delta_{ped}$  [shown in Fig. 6(a)]. For safety, we gradually reduce the input amplitude

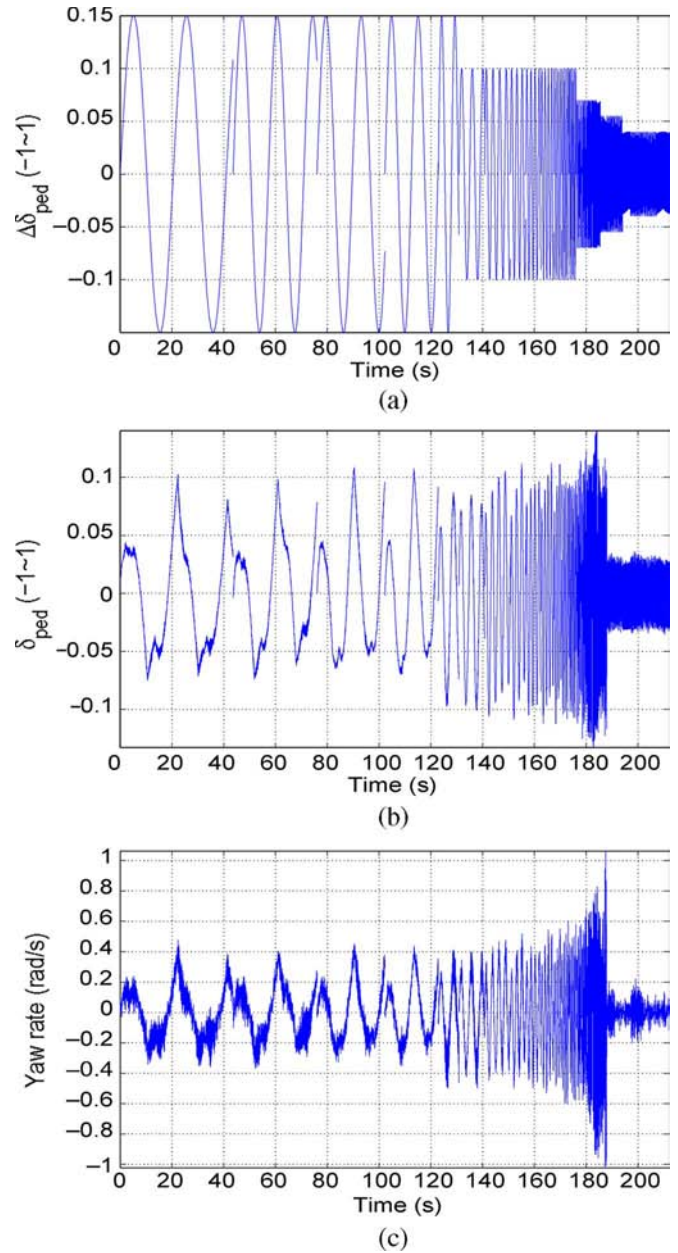


Fig. 6. Experimental data for system identification of the yaw channel. (a) Sinusoidal signals with frequency ranging from 0.05 to 20 Hz. (b) The resulting input to the yaw channel. (c) The resulting output of the yaw channel.

as the frequency increase to avoid drastic motions in the yaw channel. The resulting signals  $\{\delta_{ped}, \omega\}$  shown, respectively, in Fig. 6(b) and (c) are then used for system identification.

Black-box state-space model is selected to represent the SISO yaw-channel dynamics. The prediction-error method (PEM) [15], which is commonly used in system-identification area, is adopted as the identification algorithm. In PEM, the unknown parameter set is estimated by minimizing the sum of squared prediction error at all sampled points. To achieve the optimized identified result, the state-space models with the order from two to seven are identified and then compared with the real measured frequency response. We find that a fourth-order model, given by

$$\dot{x} = A_{yaw}x + B_{yaw}\delta_{ped}, \quad \omega = C_{yaw}x \quad (3)$$

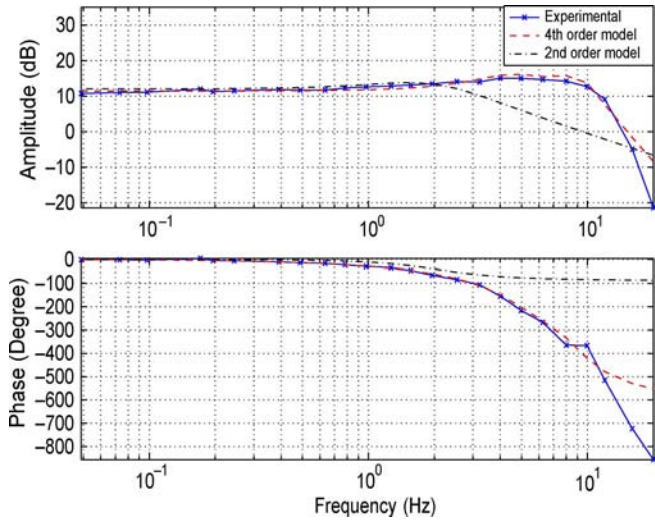


Fig. 7. Frequency-domain verification of the fourth-order model of the yaw channel.

with

$$A_{yaw} = \begin{bmatrix} -2.6571 & 21.9350 & 3.8290 & 6.0497 \\ -31.0290 & -3.5154 & 17.0990 & -3.0897 \\ 6.1059 & -6.9623 & -9.7553 & -96.3750 \\ 17.1690 & 25.7330 & 37.1760 & -33.0820 \end{bmatrix}$$

$$B_{yaw} = \begin{bmatrix} 0.6258 \\ 6.2175 \\ -29.1990 \\ -14.6430 \end{bmatrix}$$

and

$$C_{yaw} = [15.3190 \quad -10.3210 \quad 0.7307 \quad -4.7274]$$

yields the best agreement in frequency domain with the fitness of 65.48% and is finally selected as the identified model. The frequency-domain verification between the identified fourth-order model and real measured data is shown in Fig. 7. For easy reference and comparison, we also include the frequency response of the second-order model in the figure. It is clear that the identified model is much more accurate than the second-order model.

Lastly, the fidelity of the identified model is evaluated by using other sets of actual flight data, which are different from those used in the identification process. Two types of input signals are employed. The first one, shown in Fig. 8, is an automatically generated chirp signal, which covers frequencies ranging from 0.01 to 10 Hz. We note that the time-domain response of the conventional second-order model is also shown in Fig. 3 for easy reference and comparison. It clearly indicates that the identified fourth-order model yields a much more accurate response in the frequency domain. The second type of verification is to test the system responses with respect to manual-steplike signals at different input amplitudes. The result shown in Fig. 9 once again shows perfect matching between the actual measurement data and the simulated yaw rate of the fourth-order model.

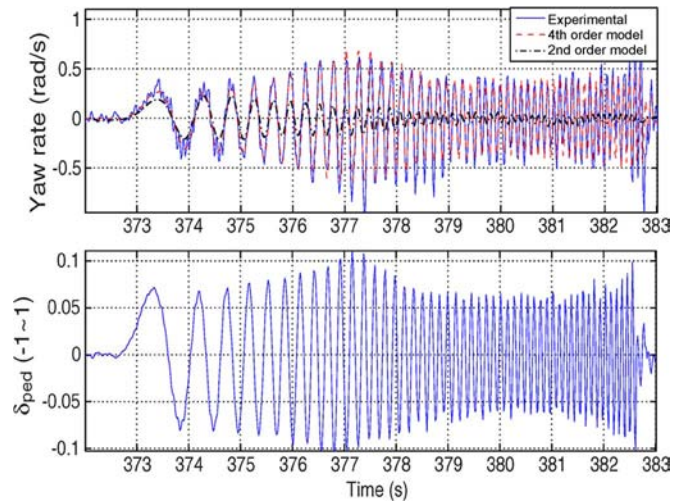


Fig. 8. Model validation using automatic chirp input signal.

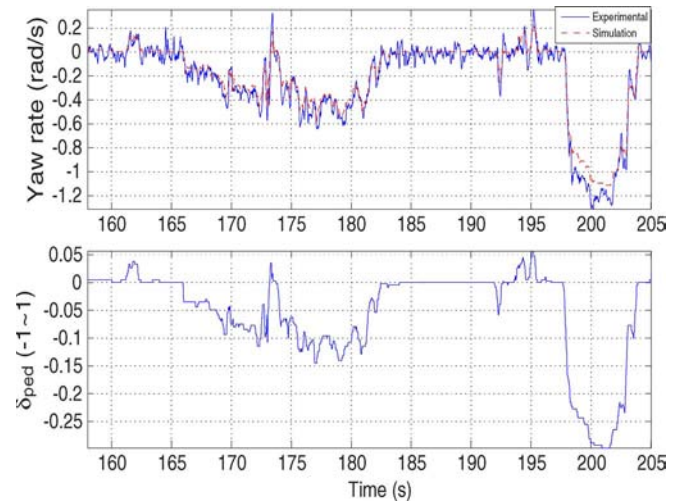


Fig. 9. Model validation using two sets of steplike input signals.

### III. CONTROL OF YAW CHANNEL USING CNF TECHNIQUE

By examining the identified model of yaw-channel dynamics, we find that the system is internally stable because of the embedded controller. The closed-loop poles of the system with the embedded controller are located at  $-12.2507 \pm j27.0777$  and  $-12.2541 \pm j57.4222$ . However, the actual performance is not good enough. This could be verified by a simple simulation experiment. We injected a step-input signal with the amplitude of 0.13. The yaw-rate output response, along with the input signal, is shown in Fig. 10. It is noticed that transient response of the overall system is pretty bad. For this reason, designing an extra control law to improve the yaw-channel performance is necessary.

We propose in this section to design a high-performance controller by using the CNF-control technique. To be more specific, we consider a linear continuous-time system  $\Sigma$  with an amplitude-constrained actuator characterized by

$$\begin{cases} \dot{x} = Ax + Bs_{\text{sat}}(u), & x(0) = x_0 \\ y = C_1 x \\ h = C_2 x \end{cases} \quad (4)$$

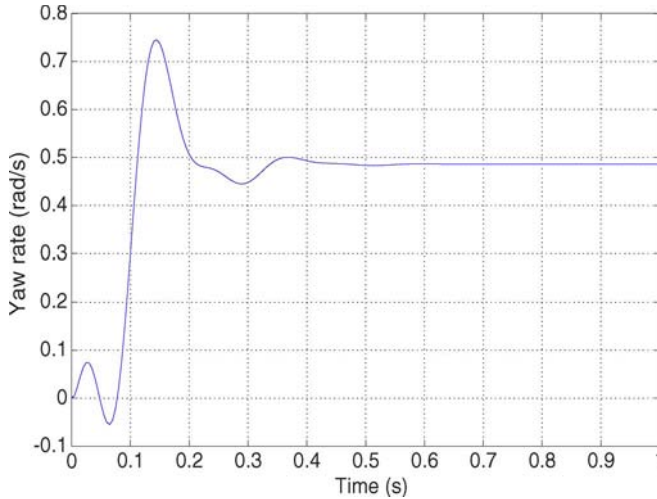


Fig. 10. Step response of the yaw channel without an additional controller.

where  $x \in \mathbb{R}^n$ ,  $u \in \mathbb{R}$ ,  $y \in \mathbb{R}^p$ , and  $h \in \mathbb{R}$  are, respectively, the state, control input, measurement output, and controlled output of  $\Sigma$ .  $A$ ,  $B$ ,  $C_1$ , and  $C_2$  are appropriate dimensional constant matrices, and  $\text{sat}: \mathbb{R} \rightarrow \mathbb{R}$  represents the actuator saturation defined as

$$\text{sat}(u) = \text{sgn}(u) \min \{u_{\max}, |u|\} \quad (5)$$

with  $u_{\max}$  as the saturation level of the input. The following assumptions on the system matrices are required: 1)  $(A, B)$  is stabilizable; 2)  $(A, C_1)$  is detectable; and 3)  $(A, B, C_2)$  is invertible and has no invariant zeros at  $s = 0$ . The objective is to design a CNF control law that causes the output to track a high-amplitude step input rapidly without experiencing large overshoot and without the adverse actuator-saturation effects. This is done through the design of a linear-feedback law with a small closed-loop damping ratio and a nonlinear-feedback law through an appropriate Lyapunov function to cause the closed-loop system to be highly damped as the system output approaches the command input to reduce the overshoot.

In what follows, we recall from [6] and [7] the step-by-step procedure of the CNF-control design with full-order measurement feedback.

Step 1) Design a linear-feedback law

$$u_L = Fx + Gr \quad (6)$$

where  $F$  is chosen such that the following: 1)  $A + BF$  is an asymptotically stable matrix, and 2) the closed-loop system  $C_2(sI - A - BF)^{-1}B$  has certain desired properties, e.g., having a small damping ratio. We note that such an  $F$  can be designed by using methods such as the  $H_2$  and  $H_\infty$  optimization approaches. Furthermore,  $G$  is a scalar and is given by

$$G = -[C_2(A + BF)^{-1}B]^{-1} \quad (7)$$

and  $r$  is a command input. Here, we note that  $G$  is well defined because  $A + BF$  is stable, and the

triple  $(A, B, C_2)$  is invertible and has no invariant zeros at  $s = 0$ .

Step 2) Given a positive definite matrix  $W \in \mathbb{R}^{n \times n}$ , we solve the following Lyapunov equation:

$$(A + BF)'P + P(A + BF) = -W \quad (8)$$

for  $P > 0$ . Such a solution is always existent, as  $A + BF$  is asymptotically stable. The nonlinear-feedback portion of the enhanced CNF control law  $u_N$  is given by

$$u_N = \rho(e)B'P(x - x_e) \quad (9)$$

where  $\rho(e)$ , with  $e = h - r$  as the tracking error, is a smooth and nonpositive function of  $|e|$ . It is used to gradually change the system closed-loop damping ratio to yield a better tracking performance. The choices of the design parameters,  $\rho(e)$  and  $W$ , will be discussed later. Next, we define

$$\begin{aligned} G_e &:= -(A + BF)^{-1}BG \\ x_e &:= G_e r. \end{aligned} \quad (10)$$

If all the state variables of the system are available for feedback, the CNF control law is given by

$$u = u_L + u_N = Fx + Gr + \rho(e)B'P(x - x_e). \quad (11)$$

Step 3) For the case when there is only a partial measurement available, the state-feedback CNF control law of (11) should be replaced by the following measurement feedback controller:

$$\begin{cases} \dot{x}_v = (A + KC_1)x_v - Ky + B\text{sat}(u) \\ u = F(x_v - x_e) + Hr + \rho(e)B'P(x_v - x_e) \end{cases} \quad (12)$$

where  $K$  is the full-order observer gain matrix such that  $A + KC_1$  is stable and

$$H = [1 - F(A + BF)^{-1}B]G. \quad (13)$$

The following result is due to [6] and [7].

*Theorem 3.1:* Given a positive definite matrix  $W \in \mathbb{R}^{n \times n}$ , let  $P > 0$  be the solution to the Lyapunov equation

$$(A + BF)'P + P(A + BF) = -W. \quad (14)$$

Given another positive definite matrix  $W_Q \in \mathbb{R}^{n \times n}$  with

$$W_Q > F'B'PW^{-1}PBF \quad (15)$$

let  $Q > 0$  be the solution to the Lyapunov equation

$$(A + KC_1)'Q + Q(A + KC_1) = -W_Q. \quad (16)$$

Note that such  $P$  and  $Q$  exist as  $A + BF$ , and  $A + KC_1$  are asymptotically stable. For any  $\delta \in (0, 1)$ , let  $c_\delta$  be the largest positive scalar such that for all

$$\begin{pmatrix} x \\ x_v \end{pmatrix} \in \mathbf{X}_{F\delta} := \left\{ \begin{pmatrix} x \\ x_v \end{pmatrix} : \begin{pmatrix} x \\ x_v \end{pmatrix}' \begin{bmatrix} P & 0 \\ 0 & Q \end{bmatrix} \begin{pmatrix} x \\ x_v \end{pmatrix} \leq c_\delta \right\} \quad (17)$$

we have

$$\left| [F \quad F] \begin{pmatrix} x \\ x_v \end{pmatrix} \right| \leq u_{\max}(1 - \delta). \quad (18)$$

Then, there exists a scalar  $\rho^* > 0$  such that, for any nonpositive function  $\rho(e)$ , locally Lipschitz in  $e$ , and  $|\rho(e)| \leq \rho^*$ , the full-order measurement CNF control law of (12) drives the system-controlled output  $h(t)$  to track asymptotically a step command input of amplitude  $r$  from an initial state  $x_0$ , provided that  $x_0$ ,  $x_{v0} = x_v(0)$ , and  $r$  satisfy

$$|Hr| \leq \delta \cdot u_{\max} \quad \begin{pmatrix} x_0 - x_e \\ x_{v0} - x_0 \end{pmatrix} \in \mathbf{X}_{F\delta}. \quad (19)$$

We note that the freedom to choose the function  $\rho$  in the CNF design is used to tune the control laws so as to improve the performance of the closed-loop system as the controlled output  $h$  approaches the set point  $r$ . Since the main purpose of adding the nonlinear part to the CNF controller is to shorten the settling time or, equivalently, to contribute a significant value to the control input when the tracking error  $e$  is small. The nonlinear part, in general, is set in action when the control signal is far away from its saturation level, and thus, it does not cause the control input to hit its limits. The following nonlinear function proposed in [6] and [7] meets such a requirement:

$$\rho(e) = -\beta |\exp(-\alpha|e|) - \exp(-\alpha|e(0)|)| \quad (20)$$

where  $\alpha$  and  $\beta$  are tuning parameters that can be adjusted to yield a desired performance.

In what follows, we adopt the aforementioned CNF-control technique to design the controller for yaw-channel dynamics that yields a top-level performance specified by the United States Army Aviation and Missile Command in [1]. It follows from the previous section that the identified fourth-order yaw dynamical model can be written as that in (4) with

$$A = \begin{bmatrix} -2.6571 & 21.9350 & 3.8290 & 6.0497 \\ -31.0290 & -3.5154 & 17.0990 & -3.0897 \\ 6.1059 & -6.9623 & -9.7553 & -96.3750 \\ 17.1690 & 25.7330 & 37.1760 & -33.0820 \end{bmatrix}$$

$$B = \begin{bmatrix} 0.6258 \\ 6.2175 \\ -29.1990 \\ -14.6430 \end{bmatrix}$$

and  $y = h = \omega = C_1x = C_2x$  with

$$C_1 = C_2 = [15.3190 \quad -10.3210 \quad 0.7307 \quad -4.7274].$$

For safety consideration, the maximal amplitude of the pedal input is kept within  $\pm 0.4$ . It is straightforward to verify that  $(A, B)$  is controllable and  $(A, C_1)$  is observable. Furthermore, the triple  $(A, B, C_2)$  is invertible with three unstable invariant zeros at  $29.013 \pm j29.572$  and  $990.68$ . We note that the nonminimum-phase property of the yaw channel can also be observed from the undershoots of its step response shown in Fig. 10, and this nonminimum-phase nature of the yaw

channel gives lots of troubles in designing a high-performance controller.

Next, we proceed to design a CNF control law for this system. Our main goal is to reduce the overshoot of the time-domain response. Since the identified model of the yaw channel with the embedded controller is stable with two pairs of poles having very small damping ratios (0.47 and 0.22), we can safely choose the state-feedback gain for the linear part of the CNF control law as  $F = 0$ , which yields

$$G = -[C_2(A + BF)^{-1}B]^{-1} = 0.2675 \quad (21)$$

and

$$G_e = -(A + BF)^{-1}BG = \begin{bmatrix} 0.0560 \\ 0.0217 \\ -0.0054 \\ -0.0785 \end{bmatrix}. \quad (22)$$

Choosing a positive definite matrix  $W = I$  and solving the Lyapunov equation  $A'P + PA = -W$ , we obtain a positive definite solution

$$P = \begin{bmatrix} 0.1071 & 0.0189 & 0.0184 & 0.0151 \\ 0.0189 & 0.0771 & 0.0306 & -0.0168 \\ 0.0184 & 0.0306 & 0.0364 & -0.0199 \\ 0.0151 & -0.0168 & -0.0199 & 0.0773 \end{bmatrix}. \quad (23)$$

For the full order, we choose an observer gain matrix

$$K = \begin{bmatrix} 1.2016 \\ 4.0081 \\ -2.9073 \\ 5.4800 \end{bmatrix} \quad (24)$$

which places the observer poles, i.e., the eigenvalues of  $A + KC_1$ , at  $-24 \pm j14.6$  and  $-26 \pm j14.6$ . Finally, we obtain a full-order measurement-feedback CNF control law

$$\dot{x}_v = \begin{bmatrix} 15.7502 & 9.5333 & 4.7070 & 0.3693 \\ 30.3711 & -44.8830 & 20.0277 & -22.0376 \\ -38.4310 & 23.0439 & -11.8797 & -82.6310 \\ 101.1171 & -30.8261 & 41.1802 & -58.9882 \end{bmatrix} x_v - \begin{bmatrix} 1.2016 \\ 4.0081 \\ -2.9073 \\ 5.4800 \end{bmatrix} \omega + \begin{bmatrix} 0.6258 \\ 6.2175 \\ -29.1990 \\ -14.6430 \end{bmatrix} \text{sat}(\delta_{\text{ped}}) \quad (25)$$

and

$$\delta_{\text{ped}} = \rho(e) ([-0.5745 \quad -0.1570 \quad -0.5716 \quad -0.6469]x_v + 0.0183r) + 0.2675r \quad (26)$$

with

$$\rho(e) = -9.6 |\exp(-1.05|e|) - 20.3679|. \quad (27)$$

#### IV. SIMULATION AND IMPLEMENTATION RESULTS

Before implementing the CNF control law on the actual UAV helicopter, we evaluate its performance through an intensive simulation process. In order to compare the overall performance

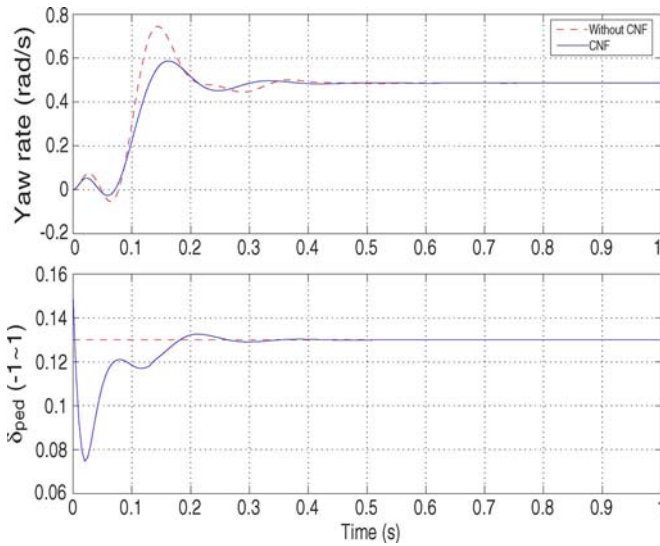


Fig. 11. Step responses of the yaw channel with and without CNF control.

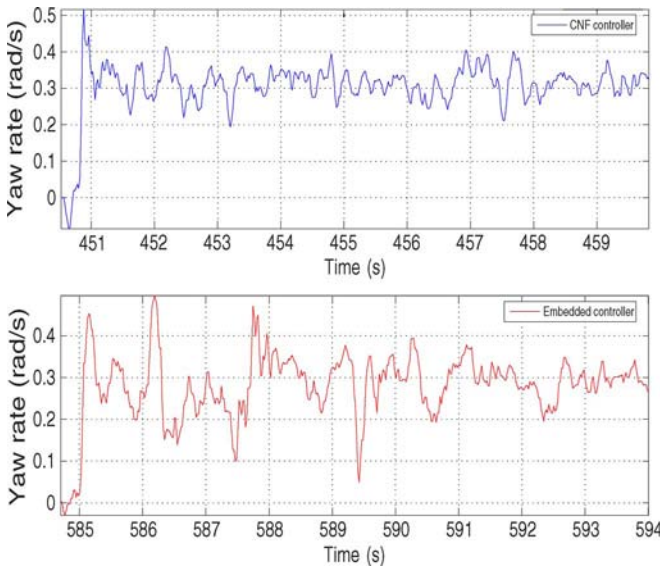


Fig. 12. Responses of the system with and without the CNF controller in actual flight tests.

of the yaw channel with and without the additional CNF controller, we choose a step reference of 0.5 rad/s. The simulation result is shown in Fig. 11. It is clear that the CNF control yields a better performance.

In what follows, we proceed to examine the performance analysis for the overall system with the CNF controller on the actual UAV helicopter. It is done by replacing the control law for the yaw channel as given in [5] with the one given in (25) and (26). The rest of the control system in [5] remains unchanged throughout the whole experimental test.

We first present the automatic-hovering-turn tests for the yaw channel on the UAV system. Fig. 12 shows the results of actual responses of the yaw channel with and without the additional CNF controller. In the actual flight test, the set point is chosen to be 0.3 rad/s. We note that the overshoot levels are slightly different with the simulation results. This is practically acceptable, and it is mainly due to mechanical friction and external environmental factors such as the precision

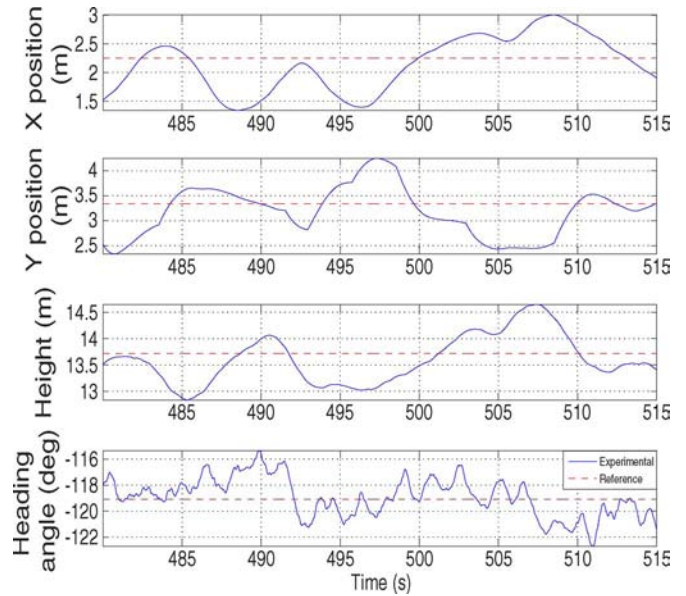


Fig. 13. Flight test. Automatic hovering.

TABLE I  
HOVERING PERFORMANCE SPECIFICATIONS AND ACTUAL TEST RESULTS

	Desired Performance	Adequate Performance	HeLion's Performance
Stabilized Hover Duration	> 30 s	> 30 s	> 35 s
Horizontal Tolerance	≤ 3 ft	≤ 6 ft	≤ 3 ft
Altitude Tolerance	≤ 2 ft	≤ 4 ft	≤ 3 ft
Heading Angle Tolerance	≤ 5°	≤ 10°	≤ 3.7°

of the GPS measurement signals. Nonetheless, the system with the additional CNF control, once again, gives a much better performance as compared to that of the system with only the embedded controller. In particular, the system with the CNF controller is capable of tracking the set point in 0.4 s and keeping it there within  $\pm 0.1$  rad/s. On the other hand, the system with only the embedded controller needs about 5 s to reach the steady state and is only able to maintain in the target with a  $\pm 0.2$ -rad/s accuracy. The advantage of using an additional CNF control is obvious in this regard.

Next, we carry out the performance evaluation of the overall system. More specifically, we follow the standard set by the United States Army Aviation and Missile Command in [1] to examine the following: 1) the stabilization and 2) the agility of the overall flight control system.

### A. Stabilization Test

The stabilization test examines the hovering stability and the accuracy of heading-hold. The performance is categorized by two levels [1], namely, the desired performance and adequate performance. The result of the actual automatic-hovering test for a duration of 35 s is shown in Fig. 13. The stabilization test results, together with the standards, are summarized in Table I. It is once again clear that our design is very successful in this category. We would like to further note that the position errors in our actual test results are mainly due to the inaccuracy of

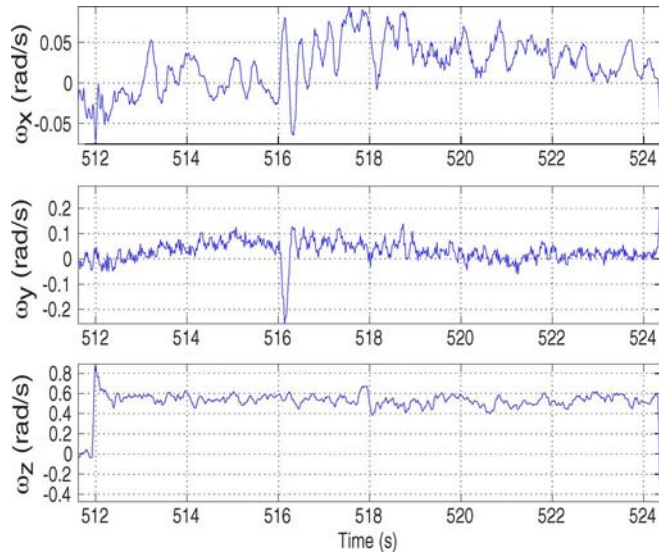


Fig. 14. Agility test. Angular rates.

TABLE II  
AGILITY PERFORMANCE SPECIFICATIONS AND ACTUAL TEST RESULT

	Level 1 Performance	Level 2 and 3 Performance	HeLion's Performance
Required Yaw Rate	> 22 deg/s	> 9.5 deg/s	> 31 deg/s

the GPS signals received. The positioning accuracy of the GPS receiver is 3 m.

### B. Agility Test

In the agility test, the UAV helicopter is required to perform a 360° self-rotation around its main shaft with a required yaw rate. The performance is categorized into three levels. The actual test results are shown in Fig. 14, in which the yaw rate is maintained at 31°/s, and summarized in Table II with the specifications set in the Aeronautical Design Standard Performance Specification Handling Qualities Requirements for Military Rotorcraft [1]. Our HeLion has again achieved a Level 1 performance in this test.

## V. CONCLUSION

We have carried out a systematic study on the yaw channel of a UAV helicopter in this paper. In particular, we have obtained a fairly accurate model for the channel with an embedded controller and improved its performance by augmenting an additional control law using the newly developed CNF-control technique. Our design has achieved a top-level performance in accordance with the standard set by the United States Army Aviation and Missile Command for Military Rotorcraft. Finally, we note that it is observed from this paper that the yaw channel of the helicopter is of nonminimum phase, which may be due to the poorly design embedded controller. Such a nonminimum-phase property generally makes it hard to further improve its control performance. This paper suggests that there is a need to redesign the embedded controller in the yaw channel. It is worth investigating the use of other type of control techniques (see, e.g., [11]) to yield a better performance.

## REFERENCES

- [1] ADS-33E-PRF, "Aeronautical design standard performance specification handling qualities requirements for military rotorcraft," United States Army Aviation Missile Command, Huntsville, AL, 2000.
- [2] P. Baranyi and Y. Yam, "Case study of the TP-model transformation in the control of a complex dynamic model with structural nonlinearity," *IEEE Trans. Ind. Electron.*, vol. 53, no. 3, pp. 895–904, Jun. 2006.
- [3] A. Bortoff, "The University of Toronto RC helicopter: A test bed for nonlinear control," in *Proc. IEEE Conf. Control Appl.*, Kohala Coast, HI, 1999, pp. 333–338.
- [4] G. Cai, K. Peng, M. Chen, and H. Lee, "Design and assembling of a UAV helicopter system," in *Proc. 5th Int. Conf. Control Autom.*, Budapest, Hungary, 2005, pp. 697–702.
- [5] G. Cai, M. Chen, K. Peng, M. Dong, and H. Lee, "Modeling and control system design for a UAV helicopter," in *Proc. 14th Mediterranean Conf. Control Autom.*, Ancona, Italy, 2006, pp. 600–606.
- [6] B. M. Chen, T. H. Lee, K. Peng, and V. Venkataramanan, "Composite nonlinear feedback control for linear systems with input saturation: Theory and an application," *IEEE Trans. Autom. Control*, vol. 48, no. 3, pp. 427–439, Mar. 2003.
- [7] B. M. Chen, T. H. Lee, K. Peng, and V. Venkataramanan, *Hard Disk Drive Servo Systems*, 2nd ed. New York: Springer-Verlag, 2006.
- [8] G. Cheng, K. Peng, B. M. Chen, and T. H. Lee, "Improving transient performance in tracking general references using composite nonlinear feedback control and its application to high-speed XY-table positioning mechanism," *IEEE Trans. Ind. Electron.*, vol. 54, no. 2, pp. 1039–1051, Apr. 2007.
- [9] M. Dong, B. M. Chen, G. Cai, and K. Peng, "Development of a real-time onboard and ground station software system for a UAV helicopter," *AIAA J. Aerosp. Comput., Inf., Commun.*, vol. 4, pp. 933–955, 2007.
- [10] V. Gavrilets, A. Shterenberg, M. A. Dahleh, and E. Feron, "Avionics system for a small unmanned helicopter performing aggressive maneuvers," in *Proc. 19th Digital Avionics Syst. Conf.*, Philadelphia, PA, 2000, pp. 1E2/1–1E2/7.
- [11] S. Goto and M. Nakamura, "Multidimensional feedforward compensator for industrial systems through pole assignment regulator and observer," *IEEE Trans. Ind. Electron.*, vol. 53, no. 3, pp. 886–894, Jun. 2006.
- [12] E. N. Johnson and S. K. Kannan, "Adaptive trajectory control for autonomous helicopters," *J. Guid. Control Dyn.*, vol. 28, no. 3, pp. 524–538, 2005.
- [13] M. La Civita, W. C. Messner, and T. Kanade, "Modeling of small-scale helicopters with integrated first-principles and system identification techniques," in *Proc. 58th Forum Amer. Helicopter Soc.*, Montreal, QC, Canada, 2002, pp. 2505–2516.
- [14] Z. Lin, M. Pachter, and S. Banda, "Toward improvement of tracking performance—nonlinear feedback for linear systems," *Int. J. Control*, vol. 70, no. 1, pp. 1–11, May 1998.
- [15] L. Ljung, *System Identification—Theory for the User*, 2nd ed. Upper Saddle River, NJ: Prentice-Hall, 1999.
- [16] B. Mettler, *Identification Modeling and Characteristics of Miniature Rotorcraft*. Norwell, MA: Kluwer, 2003.
- [17] R. W. Prouty, *Helicopter Performance, Stability and Control*. Alabar, FL: Krieger, 1990.
- [18] S. Saripalli, J. F. Montgomery, and G. S. Sukhatme, "Visually guided landing of an unmanned aerial vehicle," *IEEE Trans. Robot. Autom.*, vol. 19, no. 3, pp. 371–381, Jun. 2003.
- [19] D. H. Shim, H. J. Kim, and S. Sastry, "Control system design for rotorcraft-based unmanned aerial vehicle using time-domain system identification," in *Proc. IEEE Conf. Control Appl.*, Anchorage, AK, 2000, pp. 808–813.
- [20] M. Sugeno, I. Hirano, S. Nakamura, and S. Kotsu, "Development of an intelligent unmanned helicopter," in *Proc. IEEE Int. Conf. Fuzzy Syst.*, Yokohama, Japan, 1995, pp. 33–34.



**Guowei Cai** (S'06) was born in Tianjin, China, on June 14, 1980. He received the B.E. degree in electrical and electronics engineering from Tianjin University, Tianjin, China, in 2002. He is currently working toward the Ph.D. degree in the Department of Electrical and Computer Engineering, National University of Singapore, Singapore.

From 2002 to 2003, he was a Product Engineer with Motorola Electronic Company Ltd., Tianjin. His current research interests include system modeling and identification, control applications, and the development of unmanned-aerial-vehicle helicopter systems.



**Ben M. Chen** (S'89–M'92–SM'00–F'07) was born in Fuqing, China, in 1963. He received the B.S. degree in computer science and mathematics from Xiamen University, Xiamen, China, in 1983, the M.S. degree in electrical engineering from Gonzaga University, Spokane, WA, in 1988, and the Ph.D. degree in electrical and computer engineering from Washington State University, Pullman, in 1991.

From 1992 to 1993, he was an Assistant Professor with the Electrical Engineering Department, State University of New York, Stony Brook. Since 1993,

he has been with the Department of Electrical and Computer Engineering, National University of Singapore, Singapore, where he is currently a Professor. His current research interests include systems theory, robust control, and the development of unmanned-aerial-vehicle helicopter systems. He is the author/coauthor of seven research monographs including *Linear Systems Theory: A Structural Decomposition Approach* (Birkhäuser, 2004; Chinese edition published by Tsinghua University Press, 2008); *Hard Disk Drive Servo Systems* (Springer, 1st Edition 2002, 2nd Edition 2006); and *Robust and  $H_\infty$  Control* (Springer, 2000).

Dr. Chen is currently serving as an Associate Editor of *Control and Intelligent Systems*, *Systems and Control Letters*, *Automatica*, and several other journals. He was an Associate Editor for the IEEE TRANSACTIONS ON AUTOMATIC CONTROL.



**Kemao Peng** (A'02–M'04) was born in Anhui Province, China, in 1964. He received the B.Eng. degree in aircraft control systems, the M.Eng. degree in guidance, control, and simulation, and the Ph.D. degree in navigation, guidance, and control from Beijing University of Aeronautics and Astronautics, Beijing, China, in 1986, 1989, and 1999, respectively.

From 1998 to 2000, he was a Postdoctoral Research Fellow with the School of Automation and Electrical Engineering, Beijing University of Aeronautics and Astronautics. From 2000 to 2006, he was a Research Fellow with the Department of Electrical and Computer Engineering, National University of Singapore, Singapore, where, since 2006, he has been a Research Scientist with Temasek Laboratories. His current research interests include nonlinear-system control methods, robust control, and flight-control design. He is a coauthor of a monograph, *Hard Disk Drive Servo Systems* (Springer, 2nd Edition 2006).

Dr. Peng was the recipient of the Best Industrial Control Application Prize at the 5th Asian Control Conference, Melbourne, Australia, in 2004.



**Miaobo Dong** was born in October 1976. He received the Ph.D. degree in control science and technology from Zhejiang University, Hangzhou, China, in 2002.

From 2002 to 2004, he was a Postdoctoral Research Fellow with the State Key Laboratory of Intelligent Technology and Systems, Tsinghua University, Shenzhen, China. From 2005 to 2007, he was a Research Fellow with the Department of Electrical and Computer Engineering, National University of Singapore, Singapore. His areas of interest are the

development of software systems for unmanned aerial vehicles, intelligent control, software-enabled control, and autonomous control.



**Tong H. Lee** (M'88) received the B.A. degree (with first class honors) in the engineering tripos from Cambridge University, Cambridge, U.K., in 1980, and the Ph.D. degree from Yale University, New Haven, CT, in 1987.

He is currently a Professor with the Department of Electrical and Computer Engineering, National University of Singapore, Singapore. His research interests are in the areas of adaptive systems, knowledge-based control, intelligent mechatronics, and computational intelligence. He has coauthored

three research monographs. He is the holder of four patents (two of which are in the technology area of adaptive systems and the other two are in the area of intelligent mechatronics).

Dr. Lee was the recipient of the Cambridge University Charles Baker Prize in Engineering and the 2004 ASCC (Melbourne) Best Industrial Control Application Paper Prize. He currently holds Associate Editor appointments with *Control Engineering Practice*, *International Journal of Systems Science*, and *Mechatronics Journal*. He is currently an Associate Editor for the IEEE TRANSACTIONS ON SYSTEMS, MAN, AND CYBERNETICS and the IEEE TRANSACTIONS ON INDUSTRIAL ELECTRONICS.